Chapter 2

Mathematical and Numerical Foundations

This chapter introduces the mathematical modeling of the physical flow phenomena and the numerical processing on discretizing the governing partial differential equations. In Section 2.1, the conservation laws of mass and momentum are presented. Different strategies of solving the governing equations are compared in Section 2.2. The ensemble-average concept and its application are described in Section 2.3. Section 2.4 reviews the turbulence models that are generally applied to the closure problem of the ensemble-averaged Navier-Stokes equations. In section 2.5, one can find numerical approximation methods and solution schemes. Detailed information about the numerical code is given in Section 2.6.

2.1 Governing Equations

Fluids are substances whose molecular structure offers no resistance to external shear forces. In this work, the governing equations are applied to a certain spatial region – control volume (in Eulerian method) rather than to a given mass flow (in Lagrangian method). The conservation laws of mass and momentum are the principles that an isothermal flow obeys:

$$\frac{\partial(\rho u_i)}{\partial x_i} = 0 \tag{2.1}$$

$$\frac{\partial(\rho u_i)}{\partial t} + \frac{\partial(\rho u_i u_j)}{\partial x_j} = \frac{\partial \tau_{ij}}{\partial x_j} + \rho g_i, \tag{2.2}$$

where ρ is the fluid density, u_i the velocity component in the direction x_i of the Cartesian coordinate, g_i the component of the gravitational acceleration in x_i direction, p the pressure and τ_{ij} the stress tensor. For Newtonian fluids, the stress tensor is defined as:

$$\tau_{ij} = -\left(p + \frac{2}{3}\mu div\vec{u} \right)\delta_{ij} + 2\mu D_{ij}, \tag{2.3}$$

where

$$D_{ij} = \frac{1}{2}\left(\frac{\partial u_i}{\partial x_j} + \frac{\partial u_j}{\partial x_i} \right). \tag{2.4}$$

In Equation (2.3), μ is the molecular dynamic viscosity. Equations (2.1) to (2.4) are also referred to as Navier-Stokes equations.

Simplifications can be made to the equations. In this work, the fluid is considered to be incompressible. Besides, the molecular dynamic viscosity μ and, hence, the kinematic viscosity, $\nu=\mu/\rho$, can be treated as constants. If we ignore the gravity components, the Navier-Stokes equations can be rewritten as:

$$\frac{\partial u_i}{\partial x_i} = 0 \tag{2.5}$$

$$\frac{\partial u_i}{\partial t} + \frac{\partial u_i u_j}{\partial x_j} = -\frac{1}{\rho}\frac{\partial p}{\partial x_i} + \nu \frac{\partial^2 u_i}{\partial x_j \partial x_j}. \tag{2.6}$$

Because the governing equations are non-linear second-order partial differential equations, no analytical solution exists except in special cases. The equations must be solved numerically. Some generally used numerical methods are briefly introduced in the next section.

2.2 Simulation Methods

The most accurate approach is to solve the Navier-Stokes equations without averaging or approximation other than numerical discretizations whose errors can be estimated and controlled. All of the motions contained in the flow are resolved. This approach is usually called direct numerical simulation (DNS). In order to assure that all of the significant structures of the turbulence have been captured, the domain on which the computation is performed must be at least as large as the largest turbulence eddy that is comparable to the geometry scale of the problem, and must capture all of the kinetic energy dissipation that occurs on the smallest scales, called the Kolmogoroff scale. The cost of a simulation on a homogeneous isotropic turbulence scales as Re_L^3. Here Re_L is a Reynolds number based on the magnitude of the velocity fluctuations and the integral scale. This parameter is typically about 0.01 times the macroscopic Reynolds number that engineers use to describe a flow. Since the number of grid points that can be used in a computation is limited by the processing speed and memory of the machine, DNS is possible only at relatively low Reynolds number. Moreover, the results of a DNS contain very detailed information about the flow. This can be very useful but, on the one hand, it is far more information than any engineer needs and, on the other, DNS is too expensive to be employed very often.

Large eddy simulation (LES) treats the large eddies more exactly than the small ones because the large scale motions are generally much more energetic than the small scale ones, their size and strength make them the most effective transporters of the conserved properties. The small scales are usually much weaker, and provide little transport of these properties. LES are also three dimensional, time-dependent and expensive. But it is much less costly than DNS of the same flow. LES offers undoubtedly clear predictive advantages in bluff-body aerodynamics, in which large-scale unsteadiness is a key feature. It performs well when the separation is provoked at sharp edges and when the principle features of interest are associated with the shear layer remote from the wall and are not affected by viscous wall processes. LES is much more problematic in near-wall flows, especially when the separation is induced by the wall curvature. LES continues to be very costly, typically two orders of magnitude higher than Reynolds-averaged Navier-Stokes (RANS) solution, places considerably more stringent constraints than RANS on numerical accuracy and grid quality and requires the spectral content of boundary conditions to be specified. (For further detailed information about the recent review, see e.g. Leschziner, 2001).[24]

Both DNS and LES can provide detailed information on the flow. However, the solutions to the Navier-Stokes equations are complex, non-periodic, and quasi-random. The instantaneous solution is very sensitive to the subtle changes of initial and boundary conditions. But engineers are normally interested in knowing just a few quantitative properties of a turbulent flow, such as the average forces on a surface (and, perhaps, its distribution) or the degree of mixing between two incoming streams of fluid. Using DNS or LES to compute these quantities is, to say the least, overkill, as much more time must be invested. In this sense, DNS or LES is impractical. On the contrary, RANS solution is a good compromise through which all flow quantities are observed as a sum of averaged and fluctuating parts. The averaged quantities are solved, while the fluctuating part is modeled.

2.3 Ensemble Average

Reynolds (1895) introduced the concept of decomposing the instantaneous values of velocity and pressure into average and fluctuating parts.[34] There are different ways to define them. For example, in statistically steady flow, any flow variable $\phi(x_i, t)$, which is generally a random function of position x_i and time t, can be written as the sum of a time-averaged value $\bar{\phi}(x_i)$ and a fluctuation $\phi'(x_i,t)$ about that value:

$$\phi(x_i,t)=\bar{\phi}(x_i)+\phi'(x_i,t) \tag{2.7}$$

$$\bar{\phi}(x_i)=\lim_{T\to\infty}\frac{1}{T}\int_{t_0-T/2}^{t_0+T/2}\phi(x_i,t)dt\,, \tag{2.8}$$

where T is the averaging interval. When the quantity $\phi(x_i, t)$ is a discrete function of time, the average value is redefined with the same sampling interval as

$$\bar{\phi}(x_i) = \lim_{N\to\infty} \frac{1}{N} \sum_{n=1}^{N} \phi(x_i, t_n),\ t_n = t_0 + n\Delta t\,. \tag{2.9}$$

The time averaging cannot be used if the flow is unsteady. A general type of averaging that can be applied to any type of flow is the ensemble averaging. The ensemble average of random functions of space and time is defined as the arithmetic mean over many macroscopically identical realizations of $\phi(x_i, t)$:

$$\phi(x_i,t) = \bar{\phi}(x_i,t) + \phi'(x_i,t)\,. \tag{2.10}$$

$$\bar{\phi}(x_i,t) = \lim_{M\to\infty} \frac{1}{M} \sum_{m=1}^{M} \phi^{(m)}(x_i,t). \tag{2.11}$$

$\phi^{(m)}(x_i,t)$ is the m-th realization of $\phi(x_i, t)$. For fluid flows, the macroscopically identical realization means that statistically independent flows are exposed to the same set of initial and boundary conditions. Obviously, the ensemble-averaged quantity may be time dependent.

It can be derived from above that the following relations exist:

$$\overline{\phi'}(x_i,t) = 0 \tag{2.12}$$

$$\overline{\phi'(x_i,t)\overline{\psi(x_i,t)}} = \overline{\phi'}(x_i,t)\bar{\psi}(x_i,t) = 0 \tag{2.13}$$

$$\overline{\phi(x_i,t)\psi(x_i,t)} = \bar{\phi}(x_i,t)\bar{\psi}(x_i,t) + \overline{\phi'(x_i,t)\psi'(x_i,t)}\,. \tag{2.14}$$

Applying the concept of ensemble averaging to the incompressible Navier-Stokes equations, one can decompose the velocity components and pressure as:

$$u_i(x_i,t) = \bar{u}_i(x_i,t) + u_i'(x_i,t) \tag{2.15}$$

and

$$p(x_i,t) = \bar{p}(x_i,t) + p'(x_i,t)\,. \tag{2.16}$$

The averaging procedure results in the so-called Reynolds-averaged Navier-Stokes equations of

$$\frac{\partial(\rho\bar{u}_i)}{\partial x_i} = 0 \tag{2.17}$$

$$\frac{\partial(\rho\bar{u}_i)}{\partial t} + \frac{\partial(\rho\bar{u}_i\bar{u}_j)}{\partial x_j} = -\frac{\partial\bar{p}}{\partial x_i} + \mu\frac{\partial^2\bar{u}_i}{\partial x_j\partial x_j} - \frac{\partial(\rho\overline{u_i'u_j'})}{\partial x_j}\,. \tag{2.18}$$

Their form is similar to that without averaging except the last term in (2.18). The term $-\rho\overline{u_i'u_j'}$ is called Reynolds stress. It is responsible for momentum transport by the turbulence. This term must be closed before solving the RANS equations.

It is possible to derive equations from the high-order correlations for the Reynolds stress tensor, but they contain still more (and higher-order) unknown correlations that require modeling approximations. One solution to the problem is turbulence modeling through which the unclosed terms are modeled by known averaged properties.

2.4 Turbulence Models

Turbulent mixing plays a crucial role in the determination of many engineering relevant parameters, such as the friction drag, heat transfer, flow separation, transition from laminar to turbulent, thickness of boundary layers, etc. The fundamental problem of computational fluid dynamics (CFD) simulation lies in the prediction of the effects of the turbulence.

The turbulent states that can be encountered across the whole range of industrially relevant flows are rich, complex and varied. It is natural to assume that the effect of turbulence can be represented as an increased viscosity. This leads to the eddy-viscosity model, or Bousinesq approximation that defines the turbulent shear stress in an equivalent manner to the laminar shear stress. The Reynolds stress tensor is, then, approximated by the production of an eddy viscosity and the mean strain-rate tensor:

$$-\rho\overline{u_i'u_j'} = \mu_t\left(\frac{\partial\bar{u}_i}{\partial x_j}+\frac{\partial\bar{u}_j}{\partial x_i}\right)-\frac{2}{3}\rho\delta_{ij}k\,, \tag{2.19}$$

where μ_t is the eddy viscosity and k the turbulent kinetic energy,

$$k=\frac{1}{2}\overline{u_i'u_i'}\,. \tag{2.20}$$

In contrast to the molecular viscosity, which is an intrinsic property of the fluid, the eddy viscosity depends upon the flow.

From considerations of dimension analysis and kinetic theory, the eddy viscosity is proportional to the product of a length scale and a velocity scale. Various assumptions that go into defining these scales and the type and number of equations used for this purpose establish a classification scheme within the class of eddy-viscosity methods.

2.4.1 Zero-Equation Models

Zero-equation models, or usually referred to as algebraic equations, mean that no partial differential equation is required to describe the eddy viscosity. The eddy viscosity is

modeled by known average quantities. In the simplest description, the eddy viscosity can be defined as a function:

$$\mu_t = \rho C_\mu l^2 \frac{\partial \bar{u}}{\partial y}, \tag{2.21}$$

where C_μ is a dimensionless constant. The length scale l is a prescribed function of the coordinates.

Zero-equation models are the simplest and easiest to implement among all turbulence models. They are conceptually very simple and cause rarely unexpected numerical difficulties. Computations based on the zero-equation model provide a good representation of the zero and favorable pressure-gradient flows. But they miss the adverse pressure-gradient results rather badly. Because the length scale l depends on the flow type and is usually given empirically, one-equation models are possible only for simple flows but not for separated or highly three-dimensional flows. This is a major shortcoming of these models. Furthermore, because zero-equation models are based on boundary layer concepts, significant uncertainty should be introduced into the computation. This is the main reason why these models are not normally recommended for general applications of RANS methods.

2.4.2 One-Equation Models

The difficulty in prescribing the turbulence quantities by one-equation models suggests that partial differential equations might be used. Since a minimum description of turbulence requires at least a velocity scale and a length scale, a model that derives the needed quantities from partial differential equations is a logical choice. The class of one-equation models uses such an equation for the turbulent kinetic energy k to determine the velocity scale in the eddy viscosity, whereas no further improvement is done for the length scale.

The exact transport equation for turbulent kinetic energy can be derived from the Navier-Stokes equations:

$$\frac{\partial(\rho k)}{\partial t} + \frac{\partial\left(\rho \bar{u}_j k\right)}{\partial x_j}$$

$$= \frac{\partial}{\partial x_j}\left(\mu \frac{\partial k}{\partial x_j}\right) - \frac{\partial}{\partial x_j}\left(\frac{\rho}{2}\overline{u_j' u_i' u_i'} + \overline{p' u_j'}\right) - \rho \overline{u_i' u_j'} \frac{\partial \bar{u}_i}{\partial x_j} - \mu \overline{\frac{\partial u_i'}{\partial x_k}\frac{\partial u_j'}{\partial x_k}}. \tag{2.22}$$

The terms on the left side of this equation and the first term on the right need no modeling. The second term on the right represents turbulent diffusion of kinetic energy. The third term on the right is the rate of production of turbulent kinetic energy by the mean flow, a transfer of kinetic energy from the mean flow to the turbulence. The last term on

the right is a product of the density and the dissipation. The dissipation rate ε is the quantity at which the turbulent energy is dissipated into smaller eddies.

The one-equation models approximate the transport equation for the turbulent kinetic energy as:

$$\frac{\partial(\rho k)}{\partial t}+\frac{\partial\left(\rho\bar{u}_j k\right)}{\partial x_j}=\frac{\partial}{\partial x_j}\left[\left(\mu+\frac{\mu_t}{\sigma_k}\right)\frac{\partial k}{\partial x_j}\right]+\mu_t\left(\frac{\partial\bar{u}_i}{\partial x_j}+\frac{\partial\bar{u}_j}{\partial x_i}\right)\frac{\partial\bar{u}_i}{\partial x_j}-C_\varepsilon\frac{k^{3/2}}{l}, \tag{2.23}$$

where

$$\mu_t=\rho C_\mu l\sqrt{k}\,. \tag{2.24}$$

Only a moderate advantage is gained through using such models rather than a zero-equation model. The primary difficulty is the need to specify the length scale to reach new applications. There is no natural way for the models to accommodate an abrupt change from a wall-bounded flow to a free shear flow such as near an airfoil trailing edge or beyond the trunk lid of an automobile. Furthermore, because the length scale depends on non-local quantities in geometrically complex configurations, one-equation models introduce similar uncertainties as zero-equation models.

2.4.3 Two-Equation Models

Much more general eddy-viscosity models can be proposed by the introduction of separate differential equations to the length scale and the velocity scale. They are so called two-equation models. The most popular version of two-equation models is the k-ε model:

$$\frac{\partial(\rho k)}{\partial t}+\frac{\partial\left(\rho\bar{u}_j k\right)}{\partial x_j}=\frac{\partial}{\partial x_j}\left[\left(\mu+\frac{\mu_t}{\sigma_k}\right)\frac{\partial k}{\partial x_j}\right]+P_k-\rho\varepsilon \tag{2.25}$$

$$\frac{\partial(\rho\varepsilon)}{\partial t}+\frac{\partial\left(\rho\bar{u}_j \varepsilon\right)}{\partial x_j}=\frac{\partial}{\partial x_j}\left[\left(\mu+\frac{\mu_t}{\sigma_\varepsilon}\right)\frac{\partial\varepsilon}{\partial x_j}\right]+C_{\varepsilon 1}P_k\frac{\varepsilon}{k}-\rho C_{\varepsilon 2}\frac{\varepsilon^2}{k}, \tag{2.26}$$

where

$$\mu_t=\rho C_\mu\frac{k^2}{\varepsilon} \tag{2.27}$$

$$P_k=-\rho\overline{u_i' u_j'}\frac{\partial\bar{u}_i}{\partial x_j}. \tag{2.28}$$

The model contains five constants. Their most commonly used values are:

$$C_\mu=0.09;\quad C_{\varepsilon 1}=1.44;\quad C_{\varepsilon 2}=1.92;\quad \sigma_k=1.0;\quad \sigma_\varepsilon=1.3 \tag{2.29}$$

This class of models is the best known and the mostly used in industrial applications since it is the simplest level of closure that does not require the geometry for flow regime

dependent input. Furthermore, results from this class of models are less sensitive to free stream values. They have been applied to many flows with varying degrees of success. The models perform well when the turbulence structure is close to equilibrium. However, it is known that the standard k-ε model is not suitable for predicting a flow field that includes impinging, separation, etc. and unable to respond correctly to adverse pressure gradient. This leads to poor prediction of the development of boundary layers.

It is worth pointing out that to validate the turbulence models on solving the flow structure in the near-wall sub-layer, various so-called low-Reynolds-number versions of the k-ε models have been proposed (see e.g. Jones and Launder; Launder and Sharma; Lam and Bremhorst; Chien; Speziale, Abid and Anderson and Fan, Lakshminarayava and Barnett). [17][21][19][6][42][10]

There are, certainly, other types of two-equation models. One of them is the k-ω model where ω is a frequency of the large eddies (see Wilcox, 1998[52]). A modeled transport equation is solved for ω and the length scale is determined from $k^{1/2}/\omega$. The k-ω model performs well close to the wall in boundary flows, particularly under strong adverse pressure gradients. However, the result is very sensitive to the free stream value of ω. This limits this kind of model in finding broad applications in industrial applications.

2.4.4 Other Models

The above discussed eddy-viscosity models are suitable for fairly simple states of strain, but may be inadequate for complex strain fields arising from the action of swirl, body forces or geometrical complexity. The Reynolds-stress transport models (RSTM) are based on dynamic equations for the Reynolds stress tensor itself whose exact equations can be derived from the Navier-Stokes equations. The modeling is still necessary because there are unclosed terms. Six coupled equations, together with an equation of ε for the length scale, are needed. Some examples are Launder-Reece-Rodi model, Lumley model, Speziale-Sarkar-Gatski model, et al. [20][27][43]

The RSTM models can handle complex strain and, in principle, cope with non-equilibrium flows. However, the models are complex and expensive to compute. Additionally, they require boundary conditions for each of the stress components that can be difficult to specify and give rise to the problems of convergence. Such models have not yet been widely adopted as an industrial tool.

Turbulence modeling is nowadays an active area of research. There are surely other models, such as non-linear eddy-viscosity models (NLEVM) (e.g. Apsley et al [2]) that can provide improved results in flow impingement and reattachment. However, they are still in investigation and development. In this work, only two-equation k-ε models based on the conventional eddy-viscosity concept are employed.

2.4.5 Near-Wall Treatment

Turbulent flows are significantly affected by the presence of walls. Modeling the near-wall region in turbulent flows is particularly difficult because close to the wall, the velocity diminishes rapidly and there are interactions between the fluctuating velocity normal to the wall and the other velocity components parallel to the wall, which damps turbulence, and leads to rapid changes in the turbulence kinetic energy, Reynolds stresses and the dissipation rate. Furthermore, as the eddy size decreases nearer the wall, the action of molecular viscosity on the fluid becomes more significant.

The wall no-slip condition ensures that over some region of the wall layer, viscous effects on the transport processes must be large. The representation of these processes within a CFD model raises two problems: how to account for viscous effects at the wall and how to resolve the rapid variation of flow variables which occurs within this region.

The k-ε models are primarily valid for turbulent flows far from walls. Considerations need to be given as to how to make these models suitable for wall-bounded flows. These are generally similar to the conditions applied to any scalar equations.

Near walls, two different approaches can be employed: one can solve transport equations right up to the wall, which involves a large number of small cells and a more prolonged computation, or one can prescribe some empirically known relations for the distribution of velocity, temperature and other quantities in this region. The latter approach involves so-called wall functions. The two approaches are introduced below.

2.4.5.1 Wall Function

Numerous experiments have shown that the near-wall region can be largely subdivided into three layers. The velocity profile of a turbulent boundary layer is shown in Figure 2.1.

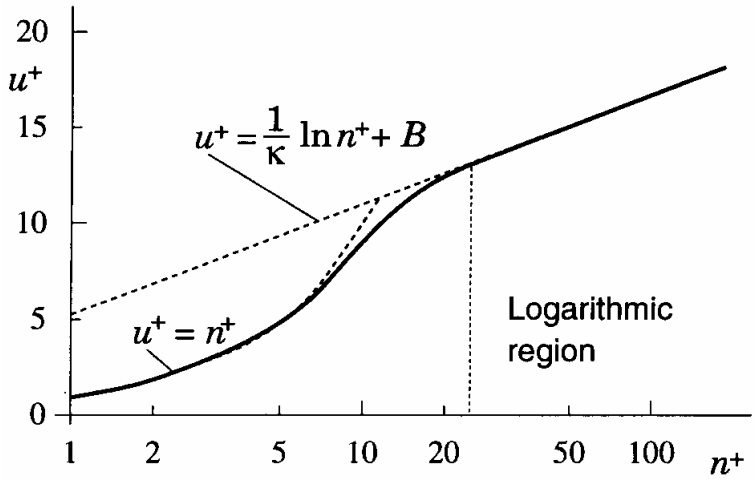

Fig. 2.1. Turbulent boundary layer: velocity profile as a function of distance normal to the wall (dashed lines are from corresponding equations, solid line represents experimental data)

The dimensionless distance from the wall n^+ (also y^+) is defined as:

$$n^+ = \frac{\rho u_\tau n}{\mu}, \tag{2.30}$$

where u_τ is the shear velocity:

$$u_\tau = \sqrt{\tau_w / \rho}. \tag{2.31}$$

τ_w is the shear stress at the wall.

In the inner layer ($0 < n^+ < 5$), called the "viscous sublayer", the flow is almost laminar, and the molecular viscosity plays a dominant role in momentum and heat or mass transfer. In the outer layer ($30 < n^+$), called the fully-turbulent layer, turbulence plays a major role. There is an interim region ($5 < n^+ < 30$) between the viscous sublayer and the fully developed turbulent layer where the effects of molecular viscosity and turbulence are equally important.

At high Reynolds number, the viscous sublayer of a boundary layer is so thin that it is difficult to use enough grid points to resolve it. This problem can be avoided by using wall functions, which rely on the existence of a logarithmic region in the velocity profile. In the method, the viscous sublayer is bridged by employing empirical formulae to provide near-wall boundary conditions for the mean flow and turbulence transport equations. These formulae connect the wall conditions (e.g. the wall shear stress) to the dependent variables at the near-wall grid node which is presumed to lie in fully-turbulent fluid. Strictly, wall functions should be applied to a point whose n^+ value is in the range $30 < n^+ < 130$.

In the logarithmic layer, the velocity profile is:

$$u^+ = \frac{\bar{u}_t}{u_\tau} = \frac{1}{\kappa} \ln n^+ + B, \tag{2.32}$$

where $\bar{u}_t$ is the mean velocity parallel to the wall, κ is the so-called von Karman constant ($\kappa = 0.41$), B is an empirical constant related to the thickness of the viscous sublayer ($B \approx 5.2$ in a flat plate boundary layer). The logarithmic velocity profile exists for simple boundary layer flows in local equilibrium.

The advantages of wall-function approach are that it escapes the need to extend the computations right to the wall, and it avoids the need to account for viscous effects in the turbulence model. In simple flows (e.g. channel and pipe flows) wall functions can

successfully improve computing times whilst giving equivalent results to low-Reynolds-number model predictions. However, in more complex and non-equilibrium flows, wall functions can give wholly unrealistic results.

The wall-function approach is not entirely satisfactory for several reasons. Most importantly, numerical solutions generally are sensitive to the point above the surface where the wall functions are used, i.e., the point where the matching occurs. Furthermore, the law of the wall does not always hold for flow near solid boundaries, most notably for separated flows.

2.4.5.2 Low-Reynolds-Number Effects

A universal near-wall behavior over a practical range of n^+ may not be realizable everywhere in a flow. Under such circumstances the wall-function concept breaks down and its use will lead to significant errors, particularly if wall friction and heat transfer rates are important. The alternative is to fully resolve the flow through to the wall by the selection of a suitable low Reynolds number wall resolving model, but the cost of the solution is around an order of magnitude greater than when a wall function is used because of the extra mesh involved.

Various so-called low-Reynolds-number versions of the k-ε models have been proposed. These models make use of damping function to achieve the asymptotic behavior near the wall.

The modified k and ε equations can be written in a common form in Cartesian tensor notation as:

$$\frac{\partial(\rho k)}{\partial t}+\frac{\partial\left(\rho\bar{u}_j k\right)}{\partial x_j}=\frac{\partial}{\partial x_j}\left[\left(\mu+\frac{\mu_t}{\sigma_k}\right)\frac{\partial k}{\partial x_j}\right]+P_k-\rho\varepsilon+\rho D \tag{2.33}$$

$$\frac{\partial(\rho\varepsilon)}{\partial t}+\frac{\partial\left(\rho\bar{u}_j \varepsilon\right)}{\partial x_j}=\frac{\partial}{\partial x_j}\left[\left(\mu+\frac{\mu_t}{\sigma_\varepsilon}\right)\frac{\partial \varepsilon}{\partial x_j}\right]+C_{\varepsilon 1} f_1 P_k \frac{\varepsilon}{k}-\rho C_{\varepsilon 2} f_2 \frac{\varepsilon^2}{k}+\rho E\,, \tag{2.34}$$

where D and E are near-wall correction functions, and f_1 and f_2 are damping functions. Some of the representative models are summarized in Table 2.1, where the local turbulent Reynolds number Re_t is defined as $\mathrm{Re}_t=k^2/(\nu\varepsilon)$.

Model	D	E	f_1	f_2	f_μ
CH*	$-2\nu k/y^2$	$2\nu\varepsilon\exp(-y^+/2)/y^2$	1	$1-0.22\exp\left[-\left(\frac{\mathrm{Re}_t}{6}\right)^2\right]$	$1-\exp(-0.0115y^+)$
JL	$-2\nu(\partial\sqrt{k}/\partial y)^2$	$2\nu\nu_t(\partial^2\bar{u}/\partial y^2)^2$	1	$1-0.3\exp\left(-\mathrm{Re}_t^2\right)$	$\exp\left[-\frac{2.5}{1+\mathrm{Re}_t/50}\right]$
LS	$-2\nu(\partial\sqrt{k}/\partial y)^2$	$2\nu\nu_t(\partial^2\bar{u}/\partial y^2)^2$	1	$1-0.3\exp\left(-\mathrm{Re}_t^2\right)$	$\exp\left[-\frac{3.4}{(1+\mathrm{Re}_t/50)^2}\right]$

Tab. 2.1. Near-wall correction and damping functions for two-equation k-ε models

*Note: CH uses non-standard k-ε constants $C_{\varepsilon 1}$=1.35, $C_{\varepsilon 2}$=1.8.

The disadvantage of low-Reynolds-number models is that a very find grid is required in each near-wall zone. Consequently, the computer-storage and runtime requirements are much greater than those of the wall-function approach. Convergence can be difficult with low-Reynolds-number k-ε models due to the problem of stiffness. Care must be taken to ensure good numerical resolution in the near-wall region so as to capture the rapid variation in variables.

2.5 Numerical Procedure

In this work, the finite volume (FV) method is employed to solve the governing equations. The FV method uses the integral form of the conservation equations as its starting point. The solution domain is subdivided into a finite number of control volumes (CVs), and the conservation equations are applied to each CV. In each CV, there is a computational node (usually the centroid) at which the variable values are to be calculated. The discretized grid defines the CV boundaries and needs not to be related to a coordinate system. The method is conservative by construction. Additionally, all terms that need to be approximated have physical meaning. These virtues make the method more popular with engineers. However, because the FV approach requires two levels of approximation: interpolation and integration, the methods of order higher than second are more difficult to develop in 3D with FV method. More descriptions can be found in Ferziger and Perić.[13]

The surface and volume integrals in the governing equations are approximated using suitable quadrature formulae. Interpolation is used to express variable values at CV surfaces. As a result, one obtains algebraic equation systems for the whole CVs. In the system, the nodal values appear and are to be solved.

2.5.1 Integrations

The generic conservation equation of (2.35) is considered as the starting point of FV method:

$$\frac{\partial}{\partial t}\int_V \rho\phi dV + \int_S \rho\phi\vec{u}\cdot\vec{n}dS = \int_S \Gamma grad\phi\cdot\vec{n}dS - \int_V q_\phi dV \ . \qquad (2.35)$$

The first term on the left side is the rate of change. The second term on the left represents the convection, and the first term on the right the diffusion. The last term on the right is the source term. In the equation, the surface and volume integrals need to be calculated. They are approximated in terms of the variable values at one or more locations on the cell surface. The cell surface values are, then, approximated in terms of the values of CV nodes.

The midpoint rule is usually applied to obtain the integrals. It is the simplest approximation and has the accuracy of second order. The surface integral can be approximated by:

$$\int_S f dS = \sum_k \int_{S_k} f dS \approx \sum_k f_k S_k \ , \tag{2.36}$$

where the integrand f can be the component of the convective ($\rho\phi\vec{u}\cdot\vec{n}$) or diffusive ($\Gamma grad\phi\cdot\vec{n}$) vector in the direction normal to the CV face. On each CV face, the integral is approximated as a product of the integral at the face centre and the cell face area. The net flux through the CV boundaries is the sum of integrals over the four (in 2D) or six (in 3D) CV faces.

Applying the midpoint rule to the volume integral, one obtains:

$$\int_V q dV \approx q_P dV \ , \tag{2.37}$$

where q_p is the value of q at the CV centre.

There are other approximations of higher order for surface or volume integral. However, because they require the integrand at locations other than cell surface centre (for surface integral) or source values at more locations than just the centre (for volume integral), higher-order approaches are more complicated, especially in 3D case. Furthermore, the overall accuracy of the approximation depends not only on the order of the integral approximation, but also on the accuracy of interpolation schemes.

2.5.2 Interpolations

The approximations to the integrals require the values of variables at locations other than the computational nodes. To calculate the convective and diffusive fluxes, the value of ϕ and its gradient normal to the cell face at one or more locations on the CV surface are needed. Volume integrals of the source term may also require the values. They have to be expressed in terms of the nodal values by interpolation.

Considered here is a typical 2D Cartesian CV arrangement whose notation is shown in Figure 2.2. Values of ϕ_e and its gradient are to be approximated.

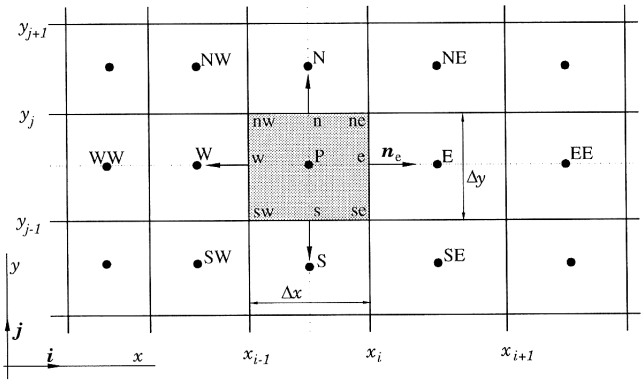

Fig. 2.2. A typical CV and the notation used for a Cartesian 2d grid

Using an upwind differencing scheme (UDS), the value of ϕ_e can be substituted by the value of its forward or backward neighboring point depending on the flow direction:

$$\phi_e = \begin{cases} \phi_P & if \quad \dot{m}_e > 0 \\ \phi_E & if \quad \dot{m}_e < 0 \end{cases}. \tag{2.38}$$

The UDS approximation is of first order accuracy and satisfies the boundedness criteria unconditionally. But it is numerically diffusive.

The central differencing scheme (CDS) interpolates linearly the value of ϕ_e between the two nearest nodes:

$$\phi_e = \phi_E \lambda_e + \phi_P (1 - \lambda_e), \tag{2.39}$$

where the factor λ_e is defined as:

$$\lambda_e = \frac{x_e - x_P}{x_E - x_P}. \tag{2.40}$$

The CDS scheme is second order accurate but may produce oscillatory solutions.

Using the linear interpolation, one can obtain the approximation of the gradient that is needed for the evaluation of diffusive fluxes:

$$\left(\frac{\partial \phi}{\partial x}\right)_e \approx \frac{\phi_E - \phi_P}{x_E - x_P}. \tag{2.41}$$

This approximation is, also, of second order accuracy.

A third order scheme is the “quadratic upwind interpolation for convective kinematics” (QUICK) method from Leonard.[23] It approximates the variable profile between P and E by a parabola instead of a straight line:

$$\phi_e = \begin{cases} \phi_P + g_1(\phi_E - \phi_P) + g_2(\phi_P - \phi_W) & if \quad \dot{m}_e > 0 \\ \phi_E + g_3(\phi_P - \phi_E) + g_4(\phi_E - \phi_{EE}) & if \quad \dot{m}_e < 0 \end{cases}. \tag{2.42}$$

Coefficients g_1 to g_4 are expressed in term of the nodal coordinates by

$$\begin{aligned} g_1 &= \frac{(x_e - x_P)(x_e - x_W)}{(x_E - x_P)(x_E - x_W)}; \quad g_2 = \frac{(x_e - x_P)(x_E - x_e)}{(x_P - x_W)(x_E - x_W)} \\ g_3 &= \frac{(x_e - x_E)(x_e - x_{EE})}{(x_P - x_E)(x_P - x_{EE})}; \quad g_4 = \frac{(x_e - x_E)(x_P - x_e)}{(x_E - x_{EE})(x_P - x_{EE})} \end{aligned} \tag{2.43}$$

Another higher-order scheme is the SMART (Sharp and Monotonic Algorithm for Realistic Transport) method. It approximates the value of ϕ_e using two points upstream and one downstream. The NVSF (Normalized Variable and Space Formulation) form of this scheme from Darwish is:[8]

$$\tilde{\phi}_e = \begin{cases} -\dfrac{\tilde{x}_e(1-3\tilde{x}_C+2\tilde{x}_e)}{\tilde{x}_c(\tilde{x}_C-1)}\tilde{\phi}_C & if \quad 0<\tilde{\phi}_C<\dfrac{\tilde{x}_C}{3} \\ \dfrac{\tilde{x}_e(1-\tilde{x}_C)}{(1-\tilde{x}_C)}+\dfrac{\tilde{x}_e(\tilde{x}_e-1)}{\tilde{x}_C(\tilde{x}_C-1)}\tilde{\phi}_C & if \quad \dfrac{\tilde{x}_C}{3}<\tilde{\phi}_C<\dfrac{\tilde{x}_C}{\tilde{x}_e}(1+\tilde{x}_e-\tilde{x}_C) \\ 1 & if \quad \dfrac{\tilde{x}_C}{\tilde{x}_e}(1+\tilde{x}_e-\tilde{x}_C)<\tilde{\phi}_C<1 \\ \tilde{\phi}_C & if \quad elsewhere \end{cases}, \qquad (2.44)$$

where the variables are normalized in the way of

$$\tilde{\phi}=\frac{\phi-\phi_U}{\phi_C-\phi_U}; \quad \tilde{x}=\frac{x-x_U}{x_C-x_U}. \qquad (2.45)$$

U, C and D are the three neighboring grid points (U and C for upstream and D for downstream) surrounding the control volume. They are W, P, E if $u_e>0$ or EE, E, P if $u_e<0$, respectively.

The SMART scheme handles the solution domain where sharp changes of ϕ and u_j in gradient or strong sources (sinks) exist. It coincides with the QUICK scheme over a large part of the monotonic range.

The interpolations of higher order can be constructed using more neighboring CV nodes. However, more computational complexity arises when these schemes are treated implicitly. Again, interpolations of higher order than third make sense only if the integrals are approximated using higher-order formulae.

2.5.3 Time Advancing

Purely steady flow fields with the time-derivative equal to zero are only a special case of the time-dependent equations. In general, fluid flows are transient. The sources for this time-dependent behavior are: external transient or non-transient forces, transient boundary conditions, moving walls (e.g. the fluttering of an airfoil), vortex stretching, a three-dimensional phenomenon due to the non-linear term of the governing equations, which also gives rise to the fluctuating nature of turbulence, and vortex shedding.

The computation of steady turbulent flow is the most common kind of simulation for the industrial use of CFD. In these cases the Reynolds-averaged flow is steady while the average turbulent quantities account for the time-dependence of the turbulent fluctuations. In this way, the RANS-equations represent the temporal average of the flow. However, the RANS-equations also allow the time-dependent Reynolds-averaged flow fields to be computed, based on the assumption that the temporal average of the turbulent quantities is not affected by the global unsteadiness. This is physically realistic when the time scale of the turbulence is much smaller than the time scales of the mean unsteadiness. A limitation is, however, that the typical turbulence frequencies are much higher than typical externally imposed or internally generated mean-flow frequencies. If the turbulence and mean flow

frequencies are in the same band, ensemble averaging looses its sense, and LES or DNS methods should be employed. A time-dependent simulation is always needed if the scale of eddies or vortices is large and is comparable to the dimensions of the geometry (e.g. the computation of a vortex-street behind bluff bodies like a car or a building).

For unsteady flow problems, the rate of change needs to be approximated. A general formulation of time-advancing schemes can be written as:

$$\frac{\rho \Delta V}{\Delta t}\left[\left(\phi^{n}-\phi^{n-1}\right)+\beta\frac{\phi^{n}-2\phi^{n-1}+\phi^{n-2}}{2}\right]+\left(F_{C}^{n}-F_{D}^{n}-Q^{n}\right)=0, \tag{2.46}$$

where the convection, diffusion and sources are treated implicitly. When the blending factor β equals to zero, one obtain the implicit Euler method of first order accuracy. When the factor is set to be unity, a three-time-level advance scheme can be obtained. It is second order accurate. Additionally, the factor can also have a value between zero and unity, which forms a blending scheme for the unsteady term.

The first order Euler scheme is unconditionally stable but not accurate for large time steps. The second order three-time-level scheme is also unconditionally stable; but requires the variables being stored in more time steps. In this work, only implicit Euler method is applied.

2.5.4 Solution Methods

The summing over the approximations of all the terms in the generic equation results in a linear algebraic equation system in which the values of ϕ at the CV nodes are unknown. The numbers of equations and unknowns equal to the number of CVs. The equation system can be written in matrix notation as:

$$A\Phi = Q, \tag{2.47}$$

where A is the square sparse coefficient matrix, Φ a vector containing the variable values at the grid nodes, and Q the vector containing all the terms that do not have unknown variable values.

The strong implicit procedure (SIP) of Stone, based on the incomplete lower-upper decomposition, becomes very effective to the sparse matrices.[44] It converges usually in a small number of iterations. The SIP method approximates the matrix A as a product of lower (L) and upper (U) triangular matrices:

$$A \approx LU - N. \tag{2.48}$$

The L and U matrices have non-zero elements only on diagonals on which A has non-zero elements. The matrix N should satisfy $N\Phi \approx 0$.

2.5.5 Pressure-Velocity Coupling

The difficulty in solving the momentum equation for incompressible flows lies in the determination of the pressure field because the pressure exists in terms of the gradient in the Navier-Stokes equations. The velocity components obtained from the momentum equation have to satisfy the continuity equation at the same time.

The difficulty can be overcome by using the SIMPLE (Semi-Implicit Method for Pressure-Linked Equation) algorithm (Caretto et al., 1972 [5]) or SIMPLEC ("C" stands for consistent) from Van Doormal and Raithby (1984).[47] The key idea is that the momentum equation can be firstly solved from known pressure field, which can be the result of the preceding iteration or a zero field. The velocity components and pressure are, then, corrected to meet the requirement of the continuity equation.

2.5.6 Boundary and Initial Conditions

The boundary and initial conditions must be given before solving the Navier-Stokes equation.

For unsteady flow, the velocity and pressure should be given as initial conditions.

At the inlet boundary, the values of the velocity components and the turbulent quantities are needed. The turbulent kinetic energy is estimated from the degree of turbulence of $k = \frac{1}{2} T_u^{\,2} u_\infty^2$ and the dissipation rate from the Kolmogorov relation ($\varepsilon \approx k^{\frac{3}{2}} / L_\varepsilon$) where L_ε is a length scale and typically a fraction of the inlet dimension.

At the outlet, a condition of zero-gradient along the grid line is used. Besides, the value of the pressure can also be imposed. The outlet boundary should be placed sufficiently far downstream from the region to avoid the "upwash".

Non-slip and impermeable conditions are imposed on the walls. The velocity components are zero. The convective fluxes are also zero.

"Moving grid" technique is necessary to simulate the flow in turbomachinery applications, in which parts of the grid move while others do not. Mass fluxes at grid faces are needed. Special treatment should be given between the moving and non-moving boundaries.

2.6 Code Description

The numerical results reported in this work are obtained by the simulation tool NS2D whose source code is provided by the research group of Prof. Schilling at Technical University of Munich in Germany.[41] The code is extended from Ferziger and Perić and has been applied to various fluid problems.[13]

The code solves two-dimensional, incompressible RANS equations with finite volume formulation. All variables are solved in their dimensionless forms and arranged in collocated grid. The code accepts block-structured grid that can be matched or unmatched at the interfaces.

Different kinds of turbulence model are implemented in the code. One can adopt either k-ε or k-ω model. Various formulations of near-wall treatment are available, including the wall function, two-layer models, and low-Reynolds-number modifications.

The code NS2D approximates the diffusive fluxes using CDS formulation. The convective fluxes can be calculated by means of UDS, CDS, QUICK or SMART algorithm. The implicit Euler method or three-time-level scheme can be adopted to advance the time step. The SIMPLE and SIMPLEC methods are ready for solving the problem of pressure-velocity coupling. SIP is the solver to the linear equation system.